Chemistry of Metals and Alloys

Chem. Met. Alloys 4 (2011) 98-106
Ivan Franko National University of Lviv
www.chemetal-journal.org

Inhibition of aluminum corrosion in acid solution by mono- and bis-azo naphthylamine dyes. Part 1

E.M. MABROUK[1,2], H. SHOKRY[1]*, K.M. ABU AL-NAJA[1]

[1] *Chemistry Department, Faculty of Applied Science, Umm-Al Qura University, Makkah, KSA*
[2] *Chemistry Department, Faculty of Science, Kafer El-Sheikh University, Kafer El-Sheikh, Egypt*
* *Corresponding author. E-mail: drheshokry@yahoo.com*

Received August 21, 2010; accepted May 18, 2011; available on-line November 8, 2011

The effect of a series of mono- and bis-azo dyes derived from dihydroxynaphthalene on the dissolution of aluminum in 2 M HCl solutions was studied using weight loss, thermometry and galvanostatic polarization techniques. The inhibition efficiency was found to increase with increasing concentration of inhibitor to reach 97.86 % for 1×10^{-4} M. The inhibition mechanism is discussed on the basis of adsorption of inhibitor molecules on the metal surface. The inhibitors were adsorbed on the surface according to the Temkin adsorption isotherm. The effect of temperature on the corrosion inhibition of Al was studied and thermodynamic functions for the dissolution and adsorption processes in the absence and in the presence of the azo dyes were computed and discussed. The results obtained from the chemical and electrochemical measurements are in good agreement.

Naphthylamineazo dye / Aluminum / Inhibitors / Weight loss / Thermometry / Polarization

1. Introduction

Aluminum and its alloys are widely used in technology because of their low density, pleasing appearance, and corrosion resistance. For these reasons, the corrosion inhibition of Al in aqueous solution has attracted the attention of many investigators [1-9]. Inhibition of metal corrosion by organic compounds is the result of adsorption of organic molecules or ions on the metal surface, forming a protective layer. This layer reduces or prevents the corrosion of the metal. The extent of adsorption depends on the nature of the metal, the condition of the metal surface, the mode of adsorption, the chemical structure of the inhibitor, and the type of corrosive media [10].

Among the numerous methods used in combating corrosion problems, the use of chemical inhibitors remains the most cost effective and practical method. The development of corrosion inhibitors based on organic compounds containing nitrogen, sulfur and oxygen atoms is of growing interest in the field of corrosion and industrial chemistry, as corrosion poses serious problems to the service lifetime of alloys used in industry [11]. The stability of the adsorbed inhibitor films formed on the metal surface to protect the metal from corrosion depends on physico-chemical properties of the molecule related to its functional groups, such as aromaticity, possible steric effects, electron density of donor atoms, as well as on the type of corrosive medium and the nature of the interaction between the inhibitor and the metal surface [12-14].

In this paper we present a first evaluation of the corrosion protection effect of mono- and bis-naphthylamineazo dyes on the dissolution of aluminum in 2 M HCl solutions by using weight loss, thermometry and polarization measurements. Thermodynamics was used to properly characterize the mechanism of the corrosion process.

2. Materials and methods

2.1 Materials

Aluminum metal with a purity of 99.94 wt.% from Aldrich having the chemical composition given in Table 1 was used in the present study. Aluminum sheets with a surface of 1 cm^2 were used for the weight loss measurements. For the thermometric measurements pieces of aluminum metal measuring 1×5 cm were used. For the polarization studies a cylindrical rod embedded in araldite with an exposed surface of 1 cm^2 was used. The electrodes in all the measurements were polished with 1-, 0- and 00-emery paper, degreased with acetone and rinsed with distilled water.

Table 1 Chemical composition of aluminum.

Element	C	Mn	P	Si	N	V	Ti	Ca	Cr	other	Al
Weight, wt.%	0.046	0.175	0.008	0.009	0.003	0.00113	0.00048	0.00006	0.0126	0.039	rest

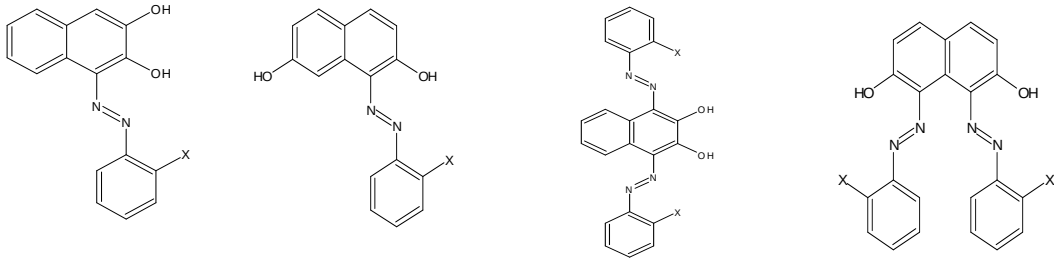

X=o-COOH (**I**), o-OCH_3 (**III**) X=o-COOH (**II**), o-OCH_3 (**IV**) X=o-COOH (**V**), o-OCH_3 (**VII**) X=o-COOH (**VI**), o-OCH_3 (**VIII**)

Fig. 1 Structural formulas of the mono- and bis-azo dyes tested for inhibition of aluminum corrosion.

2.2 Synthesis of the organic compounds

The studied mono-azo dye compounds (inhibitors) were prepared by coupling the diazonium salts of aromatic amine, o-anisidine and anthranilic acid with 0.01 mole of 2,3- and 2,7-dihydroxynaphthalenes, as described elsewhere [15]. The bis-azo dye compounds were prepared in the same manner as the mono-azo dyes, but using 0.005 mole of 2,3- and 2,7-dihydroxynaphthalenes. The prepared azo dyes were characterized by elemental analysis, IR and ^{1}H-NMR spectra. The structural formulas of the tested compounds are shown in Fig. 1.

All the chemicals used for preparing the test solutions and the azo dyes were of analytical grade (BDH, Analar) and the experiments were carried out at room temperature 30±1°C.

2.3 Methods

The weight loss measurements were carried out as described elsewhere [16,17]. The average weight loss (ΔW) for two identical experiments was taken and expressed in mg. The corrosion rate (R_{corr}) was calculated using Eq. 1:

$$R_{corr} = \frac{\Delta W(\text{mg})}{A(\text{dm}^2)\times t(\text{day})} \quad (1)$$

where A is the surface area of the specimen and t is the period of immersion in the acid solution.

The inhibition efficiency (IE) of the tested azo dyes was calculated using Eq. 2:

$$IE = \left[1-\frac{W_{add}}{W_{free}}\right]\times 100 \quad (2)$$

where W_{free} and W_{add} are the weights of the metal sheet in the absence and in the presence of the inhibitor. The degree of surface coverage (θ), which represents the part of metal surface covered by inhibitor molecules, was calculated using Eq. 3:

$$\theta = 1-\frac{W_{add}}{W_{free}} \quad (3)$$

The reaction vessel used in the thermometric measurements was basically the same as that described by Mylius [18]. The Mylius vessel was kept in a thermostat to be thermally isolated from the surrounding during the whole experiment. Exactly 15 ml of test solution was used for each experiment. The mercury reservoir of the thermometer was placed on the aluminum specimen. The variation of the temperature of the system was measured as a function of time. The term reaction number (RN) was used to represent the rate of corrosion in the absence and in the presence of the tested inhibitor. The (RN) was defined by Mylius as:

$$RN = \frac{T_m - T_i}{t} \quad (4)$$

where T_m and T_i are the maximum and initial temperatures (in °C), respectively, and t is the time in minutes elapsed to reach T_m. IE was calculated as the relative reduction of RN, using Eq. 5:

$$IE = \left[1-\frac{RN_{add}}{RN_{free}}\right]\times 100 \quad (5)$$

where RN_{free} and RN_{add} are the reaction numbers for aluminum dissolution in free and inhibited HCl solutions, respectively.

The galvanostatic polarization measurements were carried out using an EG&G model 173 potentiostat/galvanostat. A three-compartment cell

Table 2 Corrosion parameters for Al in 2 M HCl solutions containing different concentrations of azo compounds **I-VIII** as determined by the weight loss method.

Mono-azo compounds					Bis-azo compounds				
Compound	[*C*], M	*CR*, mg/dm^{3}day	*EI*	θ	Compound	[*C*], M	*CR*, mg/dm^{3}day	*IE*	θ
I	1×10^{-6}	101.81	66.94	0.7390	**V**	1×10^{-6}	59.23	84.81	0.8481
	5×10^{-6}	74.09	78.73	0.8101		5×10^{-6}	40.76	89.55	0.8955
	1×10^{-5}	63.58	82.31	0.8370		1×10^{-5}	22.64	94.19	0.9419
	5×10^{-5}	42.21	86.444	0.8918		5×10^{-5}	12.50	96.79	0.9679
	1×10^{-4}	35.14	90.99	0.9099		1×10^{-4}	6.34	97.37	0.9737
II	1×10^{-6}	128.98	73.90	0.6694	**VI**	1×10^{-6}	57.06	88.02	0.8802
	5×10^{-6}	82.97	81.01	0.7873		5×10^{-6}	38.76	91.60	0.9160
	1×10^{-5}	69.02	83.70	0.8231		1×10^{-5}	23.36	94.42	0.9442
	5×10^{-5}	52.89	89.18	0.8644		5×10^{-5}	14.67	96.33	0.9633
	1×10^{-4}	34.96	91.03	0.9103		1×10^{-4}	5.61	97.86	0.9786
III	1×10^{-6}	89.13	75.99	0.7599	**VII**	1×10^{-6}	53.80	88.02	0.8802
	5×10^{-6}	70.47	81.94	0.8194		5×10^{-6}	35.86	88.63	0.8863
	1×10^{-5}	44.74	88.53	0.8853		1×10^{-5}	17.75	94.42	0.9442
	5×10^{-5}	23.36	94.01	0.9401		5×10^{-5}	10.23	96.23	0.9623
	1×10^{-4}	17.57	95.49	0.9549		1×10^{-4}	5.07	97.86	0.9786
IV	1×10^{-6}	93.65	77.15	0.7715	**VIII**	1×10^{-6}	46.73	88.04	0.8804
	5×10^{-6}	57.24	85.32	0.8532		5×10^{-6}	34.23	90.80	0.9080
	1×10^{-5}	35.32	90.94	0.9094		1×10^{-5}	15.73	95.45	0.9545
	5×10^{-5}	21.37	94.52	0.9452		5×10^{-5}	8.33	97.35	0.9735
	1×10^{-4}	16.66	95.72	0.9572		1×10^{-4}	4.95	98.70	0.9870

with a saturated calomel reference electrode and a platinum foil auxiliary electrode was used. *IE* was calculated using the following equation:

$$IE = \left[1 - \frac{I_{add}}{I_{free}}\right] \times 100 \qquad (6)$$

where I_{free} and I_{add} are the corrosion current densities in the absence and in the presence of the tested inhibitor, respectively. The surface coverage (θ) was calculated using Eq. 7:

$$\theta = 1 - \frac{I_{add}}{I_{free}} \qquad (7)$$

3. Results and discussion

3.1 Weight loss measurements

The corrosion of pure aluminum in hydrochloric acid solutions of different concentrations using the weight loss method indicated that a molarity of 2 M of the acid was optimum for carrying out the corrosion tests. The weight loss in mg was determined in an open system at various time intervals in the absence and in the presence of different concentrations of azo compounds **I-VIII**. Fig. 2 shows the weight loss *vs.* time for azo compound **I** as a typical example of the tested azo dyes. The corrosion rate and the inhibition efficiency of Al in 2 M HCl were calculated using Eqs. 1 and 2 and the data are presented in Table 2.

From the data given in Table 2, it is clear that the corrosion rate of aluminum decreases in the presence of the inhibitors **I-VIII**, when compared to the blank. This may be due to an increase of the surface coverage of the metal by the additive molecules. Consequently the inhibition efficiency of dissolution of aluminum in hydrochloric acid solutions increases. It was found that for concentrations of the inhibitor higher than 10^{-4} M, time has little effect on the corrosion rate. This can be explained assuming that in such a solution the concentration of the inhibitor is sufficient to cover almost completely the metal surface and the rate of adsorption becomes slower, compared to that observed at lower concentrations.

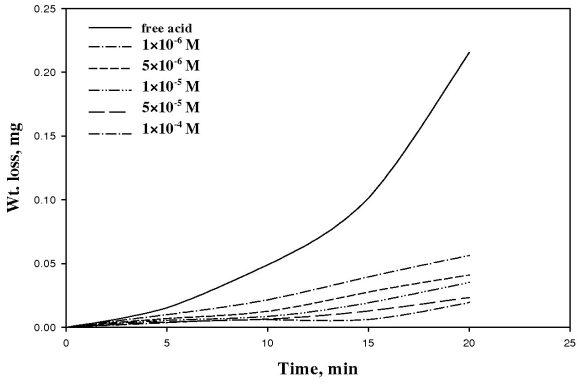

Fig. 2 The weight loss *vs.* time for aluminum corrosion in 2 M HCl in the presence of different concentrations of compound **I**.

The values of the corrosion rate and inhibition efficiency for the different azo dyes (Table 2) revealed that the decrease in corrosion rate and the increase in inhibition efficiency are more significant for the bis-azo compounds (**V-VIII**) than for the mono-azo ones (**I-IV**). This may be due to the larger size of the bis-azo molecules as compared with that of the mono-azo ones, which allows covering more surface area of the metal, as well as to the larger number of hydroxyl group which ensure strong bonding to the surface. The data also indicated that the 2,7-hydroxynaphthylazo and the o-methoxyphenylazo compounds decrease the corrosion rate, and consequently increase the inhibition efficiency, better than the 2,3-dihydroxynaphthylazo and o-carboxyphenylazo dyes. This may be connected with the ability of the electron-withdrawing carboxy group to lower the electron density on the azo group. This will destabilize the adsorption of inhibitor molecules on the metal surface, whereas the electron-donating methoxy group increases the electron density on the azo group. Besides, in the case of the carboxy group one six-membered chelate ring is available, while in the case of the methoxy group two chelate rings are available, leading to a more stable complex. The decrease of the corrosion rate and increase of the inhibition efficiency follow the sequence **VIII** > **VII** > **VI** > **V** > **IV** > **III** > **II** > **I**.

3.2 Adsorption considerations

The inhibition action of mono- and bis-azo compounds towards the corrosion of Al in 2 M HCl, can be attributed to several factors, including the number and type of adsorption sites, the nature of the inhibitor molecules, the nature of the metal surface, and the ability to form complexes [19]. The inhibition mechanism of the azo compounds under investigation is believed to be the result of adsorption of inhibitor molecules, or their metal complexes, on the surface of the metal.

Adsorption depends mainly on the charge, the nature and the electronic characteristics of the metal surface, adsorption of solvent molecules and other ionic species, temperature, and the electrochemical potential at the solution-interface [20]. Adsorption isotherms are usually used to describe the type of adsorption process. The most frequently used isotherms include those named after Langmuir, Frumkin and Temkin. The establishment of adsorption isotherms that describe the adsorption of inhibitors can provide important clues to the nature of the metal-inhibitor interaction. Adsorption of organic molecules occurs when the interaction energy between the inhibitor molecules and the metal surface is higher than that between the solvent molecules and the metal surface [21].

By far, the best fit for all of the azo compounds (**I-VIII**) was obtained with the Temkin isotherm, applying Eq. 8:

$$\exp(-2a\theta) = KC \qquad (8)$$

where a is a constant related to the molecule, θ is the degree of surface coverage, K is the equilibrium constant of the adsorption process, and C is the concentration of the inhibitor. The plot of the surface coverage θ for the azo compounds **I-VIII**, as a function of the logarithm of the inhibitor concentration, is shown in Fig. 3. Straight lines were obtained, suggesting that the Temkin isotherm is obeyed for the adsorption of these azo compounds on the aluminum surface.

Fig. 3 shows a good data fit with a high linear correlation coefficient, $R^2 \approx 0.97$. The standard free energy of the adsorption process ΔG_{ads} could be obtained from Eq. 9:

$$K = \frac{1}{55.5}\exp\left[\frac{-\Delta G_{ads}}{RT}\right] \qquad (9)$$

where 55.5 is the molar concentration of water in the solution in mol/l, R is the gas constant and T is the absolute temperature. The values of ΔG_{ads} calculated from Eq. 9 ranged from –10.52 to –10.91 kJ mol^{-1} at 30°C. The negative and relatively small values of ΔG_{ads} indicated spontaneous adsorption of the inhibitor molecules on the metal surface and physical

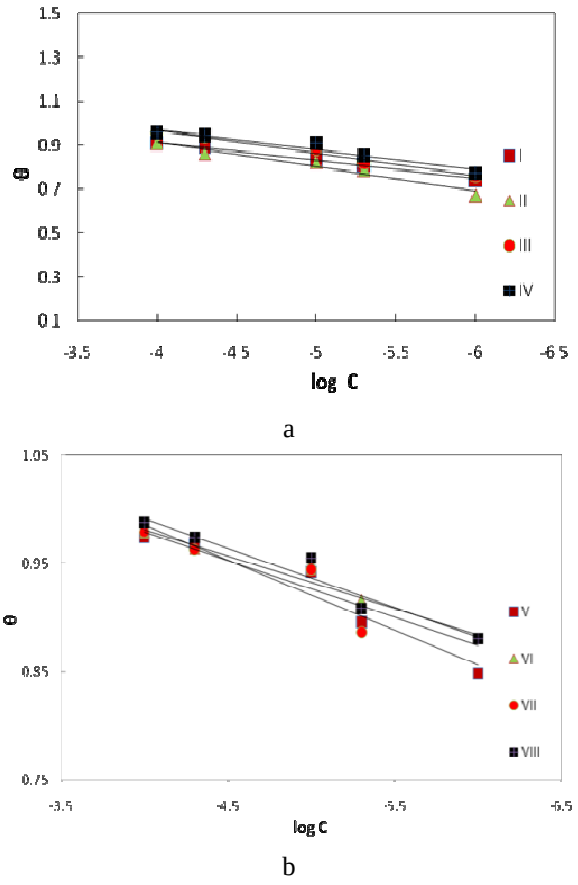

Fig. 3 Temkin adsorption isotherms of aluminum in 2 M HCl solutions: (a) inhibitors **I-IV**, (b) inhibitors **V-VIII**.

Table 3 Effect of the concentration of inhibitors **I-VIII** on the reaction number (*RN*) and the inhibition efficiency (*IE*) of aluminum in 2 M HCl solutions as determined by the thermometric technique.

Concentration,	**I**		**II**		**III**		**IV**	
M	*RN*	*IE*	*RN*	*IE*	*RN*	*IE*	*RN*	*IE*
0.00	1.1	–	1.1	–	1.1	–	1.1	–
1×10^{-6}	0.90	28.18	0.90	28.18	0.90	28.18	0.89	19.09
5×10^{-6}	0.70	36.36	0.69	37.27	0.67	39.09	0.65	40.09
1×10^{-5}	0.62	43.63	0.58	47.27	0.57	48.18	0.55	50.00
5×10^{-5}	0.57	48.18	0.51	53.63	0.49	55.45	0.49	55.45
1×10^{-4}	0.49	55.45	0.48	56.36	0.43	60.90	0.40	65.36
Concentration,	**V**		**VI**		**VII**		**VIII**	
M	*RN*	*IE*	*RN*	*IE*	*RN*	*IE*	*RN*	*IE*
0.00	1.1	–	1.1	–	1.1	–	1.1	–
1×10^{-6}	0.85	22.72	0.83	24.54	0.77	30.00	0.75	31. 81
5×10^{-6}	0.63	42.72	0.62	43.63	0.61	44.54	0.61	44.54
1×10^{-5}	0.44	60.00	0.44	60.00	0.44	60.00	0.43	60.90
5×10^{-5}	0.32	70.90	0.32	70.90	0.32	70.90	0.32	70.90
1×10^{-4}	0.31	71.81	0.30	72.72	0.30	72.73	0.29	73.63

adsorption. Values of ΔG_{ads} up to –20 kJ mol^{-1} are generally consistent with electrostatic interaction between charged molecules and a charged metal surface (which indicates physical adsorption), while values more negative than -40 kJ mol^{-1} involve charge sharing or transfer of electrons from the inhibitor molecules to the metal surface to form bonds of coordinate type (which indicates chemisorption) [22].

3.3 Thermometric measurements

The effect of the concentration of the inhibitors **I-VIII** on the thermometric curves of aluminum in 2 M HCl solutions was studied and the results obtained for compound **I** are represented graphically in Fig. 4 as an example. Similar curves (not shown) were obtained for the other compounds. As shown in Fig. 4, the curves revealed that the dissolution of aluminum in HCl solution is characterized by an initial slow rise of temperature, followed by a sharp rise, and finally a decrease after attaining a maximum value. The initial slow rise, which characterizes the first part of the thermometric curves, may be due to an oxide film originally present on the metal surface, which protected it from reaction with the medium. As the concentration of additives increases, the time required to reach the maximum temperature T_m increases and, consequently, the rate of the temperature rise decreases. The maximum temperature measured for the free acid solution was 87°C, which was attained after ≈ 45 min. The reaction numbers of the azo compounds **I-VIII** at different concentrations were calculated using Eq. 5 and the extent of corrosion inhibition by a certain concentration of the additives (*IE*) was evaluated from the relative reduction of the reaction number (*RN*), given by Eq. 6 (Table 3). The results indicated that the reaction number decreases with increasing concentration of inhibitor and consequently, the inhibition efficiency (*IE*) increases.

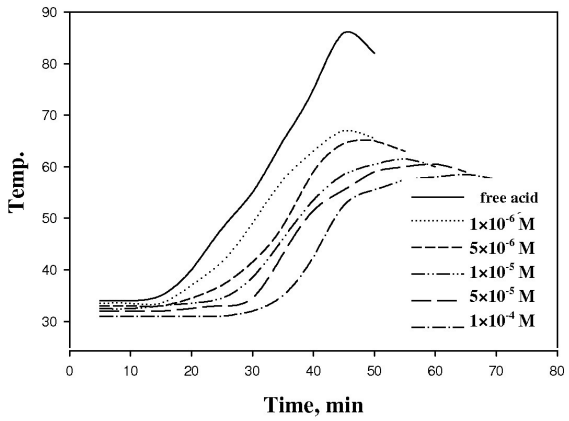

Fig. 4 Variation of temperature with time for aluminum in 2 M HCl solutions for different concentrations of compound **I**.

3.4 Galvanostatic polarization measurements

Galvanostatic polarization measurements were carried out in 0.1 M HCl solutions, in the absence and in the presence of different concentrations of the inhibitors (**I-VIII**). Fig. 5 presents cathodic and anodic polarization curves for azo compound **I**. Similar curves (not shown) were obtained for the other azo compounds. Inspection of Fig. 5 reveals that an increase of the inhibitor concentration shifts the anodic curves to more positive potentials and the cathodic curves to more negative ones. This may be ascribed to adsorption of inhibitor molecules on the corroded metal surface.

The corrosion current density (I_{corr}) was calculated by extrapolation of the anodic and cathodic Tafel lines with a steady state corrosion potential (E_{corr}). The anodic Tafel slope (β_a) and the cathodic Tafel slope (β_c) were evaluated. The inhibition efficiency (*IE*) and the surface coverage (θ) were calculated using Eqs. 6

Table 4 The effect of the concentration of inhibitors **I-VIII** on the free corrosion potential (E_{corr}), corrosion current density (I_{corr}), Tafel slopes (β_a and β_c), degree of surface coverage (θ), and inhibition efficiency (*IE*) for the corrosion of aluminum in 2 M HCl at 30°C.

Compound	Concentration, M	$-E_{corr}$, mV(SCE)	I_{corr}, μA cm^{-2}	$-\beta_c$, mV dec^{-1}	β_a, mV dec^{-1}	θ	*IE*
Blank	0	730	69.6	89	78	–	–
I	1×10^{-6}	727	50.4	103	81	0.276	27.58
	5×10^{-6}	726	44.2	103	82	0.365	36.49
	1×10^{-5}	725	41.2	104	82	0.408	40.80
	5×10^{-5}	723	37.1	108	84	0.467	46.69
	1×10^{-4}	722	33.2	110	84	0.477	47.70
II	1×10^{-6}	724	46.2	102	82	0.336	33.62
	5×10^{-6}	723	43.5	106	83	0.375	37.50
	1×10^{-5}	718	40.2	107	85	0.422	42.24
	5×10^{-5}	715	35.2	110	87	0.494	49.42
	1×10^{-4}	715	32.3	113	88	0.536	53.59
III	1×10^{-6}	723	42.2	106	83	0.394	39.36
	5×10^{-6}	722	38.6	107	88	0.445	44.54
	1×10^{-5}	722	35.4	108	91	0.491	49.13
	5×10^{-5}	718	29.2	115	93	0.580	58.04
	1×10^{-4}	715	27.2	117	94	0.609	60.91
IV	1×10^{-6}	728	40.2	90	79	0.422	42.24
	5×10^{-6}	726	36.2	91	80	0.480	47.98
	1×10^{-5}	725	33.9	93	80	0.513	51.29
	5×10^{-5}	723	28.2	103	82	0.595	59.48
	1×10^{-4}	723	26.2	104	83	0.624	62.35
V	1×10^{-6}	726	38.4	100	82	0.448	44.82
	5×10^{-6}	725	35.2	102	83	0.494	49.42
	1×10^{-5}	722	32.2	104	85	0.537	53.73
	5×10^{-5}	721	26.6	110	86	0.618	61.78
	1×10^{-4}	720	25.1	112	87	0.640	63.93
VI	1×10^{-6}	719	35.5	103	81	0.490	48.99
	5×10^{-6}	715	32.2	107	82	0.537	53.73
	1×10^{-5}	712	29.7	108	84	0.573	57.32
	5×10^{-5}	710	24.8	113	88	0.644	64.36
	1×10^{-4}	708	22.7	114	91	0.674	67.38
VII	1×10^{-6}	722	32.8	103	85	0.529	52.87
	5×10^{-6}	725	30.7	106	87	0.559	55.89
	1×10^{-5}	722	27.5	109	90	0.605	60.48
	5×10^{-5}	715	22.3	114	94	0.679	67.95
	1×10^{-4}	710	20.7	116	96	0.703	70.25
VIII	1×10^{-6}	725	30.4	102	83	0.563	56.32
	5×10^{-6}	722	28.3	105	85	0.593	59.33
	1×10^{-5}	720	25.2	108	85	0.638	63.79
	5×10^{-5}	715	20.2	112	88	0.710	70.97
	1×10^{-4}	713	18.4	114	90	0.736	73.56

and 7 and are listed in Table 4. The data given in Table 4 revealed that both β_a and β_c increase slightly with increasing concentration of the inhibitors **I-VIII**, indicating that these compounds affect both the anodic and cathodic reactions. Therefore, the hydroxynaphthaleneazo compounds **I-VIII** can be considered as mixed inhibitors. The corrosion current (I_{corr}) decreases and the inhibition efficiency (*IE*) increases with increasing concentration of inhibitor.

The values of *IE* calculated for the acid corrosion of aluminum using the three different techniques showed a good agreement and confirmed the conformity of the experimental results. The observed discrepancies could be attributed to the different experimental conditions under which each technique was carried out.

The results obtained from the three different techniques revealed that *IE* depends on the type of inhibitor (mono-azo or bis-azo), the position of the hydroxyl groups in the naphthyl ring and the type of substituent. It is clear that the corrosion rate decreases and the inhibition efficiency increases markedly in the

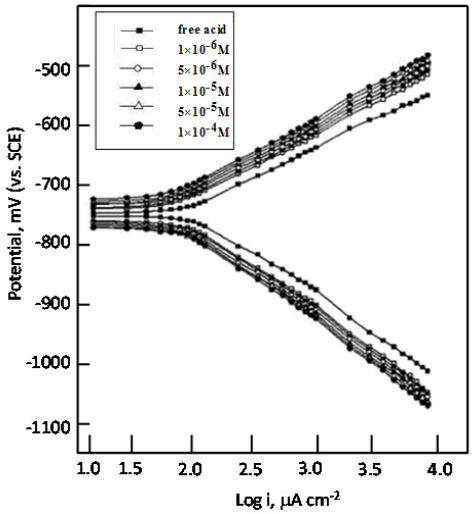

Fig. 5 Galvanostatic polarization curves for the corrosion of aluminum in 2 M HCl for different concentrations of compound **I**.

Table 5 Thermodynamic activation parameters of corrosion of aluminum in free and inhibited 2 M HCl acid solutions at 30°C.

Compd.	$-E_a$*, kJ mol^{-1}	$-\Delta H$*, kJ mol^{-1}
Free acid	44.95	42.26
I	48.74	46.06
II	54.88	52.20
III	56.21	53.53
IV	57.46	55.61
V	59.79	57.11
VI	62.14	59.45
VII	65.88	63.20
VIII	69.85	67.16

case of the bis-azo compounds, in comparison with the mono-azo ones. This may due to the larger size of the bis-azo molecule, which covers a larger surface area of the metal, as well as to the greater number of hydroxyl groups, which are strongly bonded the surface. In addition, the results indicate that the 2,7-dihydroxynaphthylazo and o-methoxyphenylazo compounds decrease the corrosion rate, and consequently increase the inhibition efficiency, more than the 2,3-dihydroxynaphthylazo and o-carboxyphenylazo compounds.

3.5 Thermodynamic considerations

The effect of temperature on the corrosion rate of Al in a 2 M HCl solution, in the absence and in the presence of 1×10^{-4} M of the selected inhibitors, was studied by weight loss measurements at 40, 50 and 60°C. It is clear that the corrosion rate increases with increasing temperature. This indicates that an increase of the temperature decreases the inhibition efficiency and the best inhibition efficiency was obtained at 40°C.

A plot of the logarithm of the corrosion rate of aluminum obtained from weight loss measurements *vs.* 1000/*T* gave straight lines, as shown in Fig. 6. The apparent activation energy (E_a*) was calculated by using the following relationship [23]:

$$r = A\exp\left[\frac{E_a^*}{RT}\right] \quad (10)$$

$$\log r = \log A - E_a^*/2.303RT \quad (11)$$

where E_a* is the apparent activation energy for the corrosion of aluminum in 2 M HCl solutions, R the general gas constant, *A* the Arrhenius pre-exponential factor and *T* is the absolute temperature. The values of E_a* obtained from the slopes of these lines are given in Table 5.

From the values of the Arrhenius constant and the activation energy, it is evident that the degree of linearity of the lines on the Arrhenius plots is very close to unity, indicating strong adherence of the experimental data to the Arrhenius theory. Secondly, the value of the activation energy for the blank solution was lower than those obtained for the solutions containing inhibitors, indicating that mono-azo and bis-azo compounds deferred the corrosion of Al in HCl solutions. Lastly, the activation energies were lower than the threshold value of 80 kJ/mol required for chemical adsorption, hence the adsorption of mono-azo and bis-azo compounds on the Al surface is consistent with a mechanism of physical adsorption.

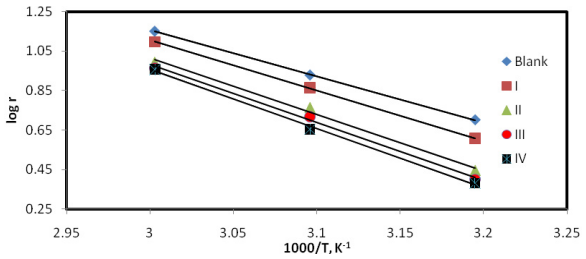

a

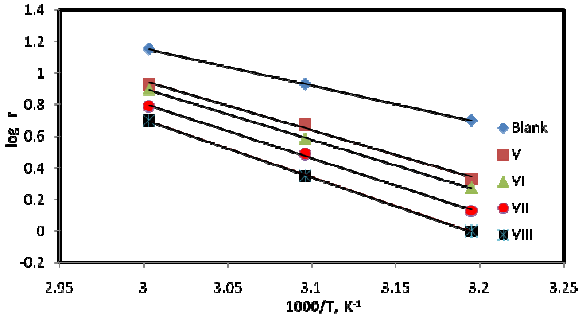

b

Fig. 6 Arrhenius plots of the corrosion rate of aluminum in 2 M HCl in the absence and in the presence of (a) inhibitors **I-IV** and (b) inhibitors **V-VIII**.

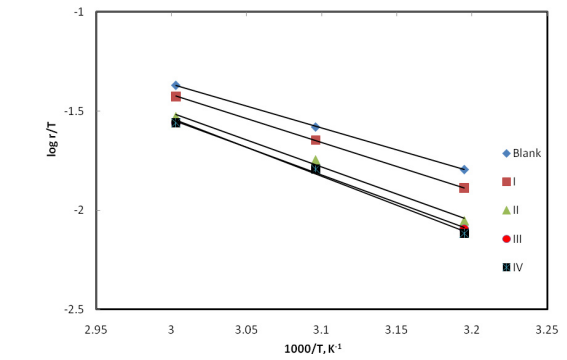

a

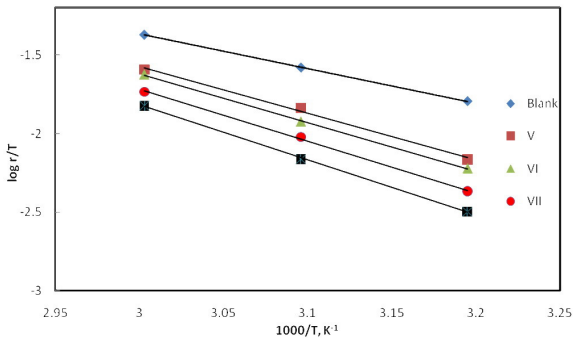

b

Fig. 7 Transition state plots of the corrosion rate of aluminum in 2 M HCl in the absence and in the presence of (a) inhibitors (**I-IV**) and (b) inhibitors (**V-VIII**).

An alternative formulation of the Arrhenius equation is the transition state equation [24]:

$$r = \frac{RT}{Nh}\exp\frac{\Delta S^*}{R}\exp\left[\frac{-\Delta H^*}{RT}\right] \qquad (12)$$

where h is the Planck constant, N the Avogadro number, ΔS^* the entropy of activation, and ΔH^* the enthalpy of activation. Rearranging and taking the logarithm of both sides of Eq. 12 yields Eq. 13:

$$\log\frac{r}{T} = \log\frac{R}{Nh} + \frac{\Delta S^*}{2.303R} - \left[\frac{\Delta H^*}{2.303RT}\right] \qquad (13)$$

According to Eq. 13, a plot of $\log(r/T)$ *vs.* $1000/T$ should produce a straight line with a slope equal to $\Delta H^*/2.303R$. Fig. 7 illustrates the general features of the plots of $\log(r/T)$ *vs.* $1000/T$, from which the values of ΔH^* listed in Table 5 were calculated. The data show that the thermodynamic activation functions (E_a^* and ΔH^*) of the corrosion of aluminum in 2 M HCl solution in the presence of the inhibitors are higher than for the free acid solutions. The adsorption of the inhibitors is assumed to occur on the higher energy sites and the presence of the inhibitor, which results in blocking of active sites, must be associated with an increase of the activation energy of aluminum corrosion in the inhibited state [25]. The values of ΔH^* are negative**,** indicating that the adsorption of the inhibitors on the surface of the metal is exothermic [26-28], and range from –42 to –67 kJ/mol at 40°C.

Conclusions

Hydroxynaphthaleneazo dye compounds inhibit the corrosion of Al in 2 M HCl solutions. The inhibition efficiency of these compounds increased with increasing concentration of the inhibitor, increasing electron donor characteristic of the substituted groups, and decreasing temperature. The inhibition action of these compounds is attributed to adsorption of inhibitor molecules on the metal surface. The adsorption process was found to obey the Temken adsorption isotherm. The order of increasing inhibition efficiency for the investigated compounds is **I** < **II** < **III** < **IV** < **V** < **VI** < **VII** < **VIII**. The additives influence both the cathodic and the anodic reactions in the HCl solution. This indicates that the additives act as mixed-type inhibitors.

References

[1] M. Abdallah, *Corros. Sci.* 46 (2004) 1981.
[2] A.Y. El-Etre, H.E. Megahed, M. Abdallah, M.A. Obied, *Corros. Prev.* 32, March (2004).
[3] S.S. Abd El-Rehim, H.H. Hassan, M.A. Amin, *Mater. Chem. Phys.* 78 (2002) 337.
[4] M.L. Zheludkevich, K.A. Yasaku, S.K. Poznyak, M.G.S. Ferreira, *Corros. Sci.* 47 (2005) 3368.
[5] M.M. Osman, S.S. Abd El-Rehim, *Mater. Chem. Phys.* 53 (1998) 34.
[6] G.K. Gomma, M.H. Wahdan, *Mater. Chem. Phys.* 39 (1995) 209.
[7] M. Abdallah, *Bull. Electrochem.* 16(6) (2000) 258.
[8] M. Abdalla, H.E. Meguhid, A.Y. El-Etre, M.A. Obied, E.M. Mabrouk, *Bull. Electrochem.* 20(6) (2004) 277.
[9] K.S. Khairou, A.A. Alfi, E.M. Mabrouk, *Mater. Sci. Res. Indian* 3(2a) (2006) 155.
[10] M.R. Saleh, A.M. Shams El-Din, *Corros. Sci.* 21(6) (1981) 439.
[11] F. Bentiss, M. Lagrence, M. Traisnel, J.C. Hornez, *Corros. Sci.* 41 (1999) 789.
[12] V.S. Sastry, *Corrosion Inhibitors, Principles and Applications*, John Wiley & Sons, New York, 1998.
[13] F. Bentiss, M. Lagrence, M. Traisnel, *Corros.* 56 (2000) 733.
[14] F. Bentiss, M. Traisnel, M. Lagrence, *J. Appl. Electrochem.* 31 (2001) 41.
[15] J.B. Conant, R.E. Lutz, B.B. Corson, *Organic Syntheses*, Coll. Vol. 1, John Wiley & Sons, New York, 1941, p. 49.

[16] P.B. Mathur, T. Vasudevan, *Corros.* 38 (1982) 17.
[17] R.J. Chin, K. Nobe, *J. Electrochem. Soc.* 118 (1971) 545.
[18] F.Z. Mylius, *Z. Metallkd.* 14 (1922) 233.
[19] A.S. Fouda, M. Mousa, F.Taha, A. El-Neanaa, *Corros. Sci.* 26 (1986) 719.
[20] I.L. Rozendeld, *Corrosion Inhibitors*, Mc Graw-Hill, New York, 1981.
[21] G. Quartarone, G. Moretti, A. Tassan, A. Zingales, *Werkst. Korros.* 45 (1994) 34.
[22] P.C. Okafor, E.E. Ebenso, U.J. Ibok, U.J. Ekpe, M.I. Ikpi, *Trans. SAEST* 38 (2003) 91.
[23] G. Trabanelli, In: F. Mansfeld (Ed.), *Corrosion Mechanisms*, Marcel Dekker, New York, 1987, p. 119.
[24] S. Sayed, E.R. Abd, H.H. Hamdy, A.A. Mohammed, *Mater. Chem. Phys.* 70 (2001) 64.
[25] A.S. Founda, A. Abd El-Aal, A.B. Kandil, *Desalination* 201 (2006) 216.
[26] E.E. Ebenso, *Mater. Chem. Phys.* 79 (2003) 58.
[27] E.E. Ebenso, *Bull. Electrochem.* 19 (2003) 209.
[28] H.M. Bhajiwala, R.T. Vashi, *Bull. Electrochem.* 17 (2001) 441.